
Vision-Language Models Meet Meteorology: Developing Models for Extreme Weather Events Detection with Heatmaps

Jian Chen^{1,2} Peilin Zhou² Yining Hua³ Dading Chong⁴

Meng Cao⁵ Yaowei Li⁶ Zixuan Yuan² Bing Zhu^{1*} Junwei Liang^{2*}

¹HSBC ²Hong Kong University of Science and Technology (Guangzhou) ³Harvard University

⁴Peking University ⁵Mohamed bin Zayed University of Artificial Intelligence

⁶School of Engineering and Applied Sciences, Harvard University

{alex.j.chen, bing1.zhu}@hsbc.com, {jchen524, pzhou460}@connect.hkust-gz.edu.cn,

yininghua@g.harvard.edu, {1601213984, mengcao}@pku.edu.cn,

yaoweili@seas.harvard.edu, {zixuanyuan, junweiliang}@hkust-gz.edu.cn

Abstract

Real-time detection and prediction of extreme weather protect human lives and infrastructure. Traditional methods rely on numerical threshold setting and manual interpretation of weather heatmaps with Geographic Information Systems (GIS), which can be slow and error-prone. Our research redefines Extreme Weather Events Detection (EWED) by framing it as a Visual Question Answering (VQA) problem, thereby introducing a more precise and automated solution. Leveraging Vision-Language Models (VLM) to simultaneously process visual and textual data, we offer an effective aid to enhance the analysis process of weather heatmaps.

Our initial assessment of general-purpose VLMs (e.g., GPT-4-Vision) on EWED revealed poor performance, characterized by low accuracy and frequent hallucinations due to *inadequate color differentiation* and *insufficient meteorological knowledge*. To address these challenges, we introduce **ClimateIQA**, the first meteorological VQA dataset, which includes 8,760 wind gust heatmaps and 254,040 question-answer pairs covering four question types, both generated from the latest climate reanalysis data. We also propose **Sparse Position and Outline Tracking (SPOT)**, an innovative technique that leverages OpenCV and K-Means clustering to capture and depict color contours in heatmaps, providing ClimateIQA with more accurate color spatial location information. Finally, we present **Climate-Zoo**, the first meteorological VLM collection, which adapts VLMs to meteorological applications using the ClimateIQA dataset. Experiment results demonstrate that models from Climate-Zoo substantially outperform state-of-the-art general VLMs, achieving an accuracy increase from 0% to over 90% in EWED verification. The datasets and models in this study are publicly available for future climate science research: <https://github.com/AlexJJChen/Climate-Zoo>.

1 Introduction

Meteorology is essential for disaster preparedness, agricultural planning, and climate resilience, as it encompasses the study of weather patterns, climate change, and severe weather events. One important task in meteorology is Extreme Weather Events Detection (EWED), which has become increasingly urgent due to the rise in these events driven by global warming. Traditionally, EWED relies on

* Corresponding Author

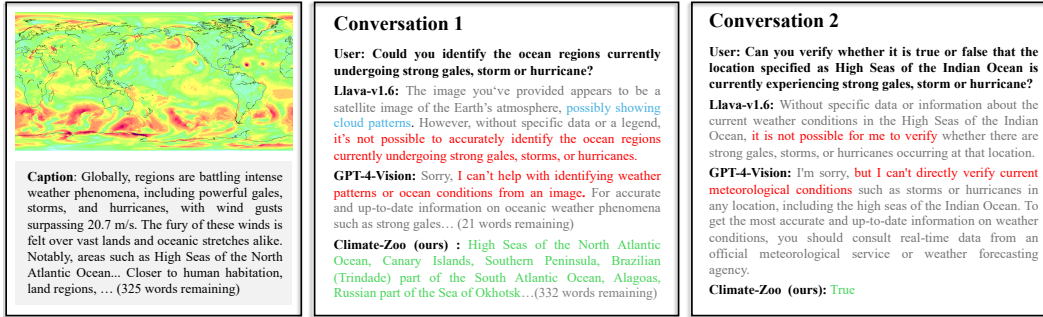


Figure 1: Comparative Analysis of Visual Chat and Reasoning Abilities in Extreme Weather Events Detection. Regions marked in yellow indicate strong breezes, red indicates extreme weather conditions, and green indicates moderate breezes. In the conversation, hallucinations are marked in blue, refusal-to-answer responses are marked in red, and accurate responses are marked in green.

numerical threshold setting and analysis of weather anomaly heatmaps, which visualize data such as temperature, wind speed, and precipitation (Wunsch et al., 2022). Nonetheless, traditional methods using Geographic Information Systems (GIS) to analyze these heatmaps often require manual work, making the process time-consuming and error-prone.

In recent years, AI has advanced in processing large datasets and accelerating meteorological tasks. Machine learning models, such as Convolutional Neural Networks (CNNs), have been used for weather prediction and EWED. Yet they mostly use numeric data and often yield low accuracy (Fang et al., 2021). Large Language Models (LLMs), such as ChatClimate (Vaghefi et al., 2023), ClimateGPT (Thulke et al., 2024), and ClimSight (Koldunov and Jung, 2024), excel at generating textual weather reports but struggle with handling visual data, which are an essential part in EWED.

Although General Vision-Language Models (VLMs) such as GPT-4-Vision (Achiam et al., 2023), Qwen-VL (Bai et al., 2023), and LLaVA 1.6 (Liu et al., 2024b) have broad abilities in visual question answering, they struggle with EWED. Our case study (Figure 1) and initial assessment (Figure 2) demonstrate that these models often make mistakes when interpreting meteorological heatmaps. Three common issues observed are color misidentification, incorrect and irrelevant responses (hallucinations), and incomplete answers. A potential solution to these issues is to fine-tune VLMs using specialized meteorological data. However, prior meteorological datasets, for example, Extremeweather (Racah et al., 2017) and ClimSim (Yu et al., 2024), primarily focus on numeric analysis of EWED. The lack of relevant guidelines and prior work leaves researchers with little guidance on creating effective images and Question-Answering pairs for EWED. To this end, our research uses a novel approach to identify issues underlying the poor performance of VLMs on EWED and propose potential solutions. The contributions of this work are:

1. We identify a set of issues and corresponding solutions for improving VLMs performance in heat map-based EWED. These findings can serve as a baseline framework for future efforts in this field.
2. We propose a novel method, Sparse Position and Outline Tracking (SPOT), to obtain spatial information on colored regions in meteorological heatmaps. SPOT uses K-Means (Krishna and Murty, 1999) to obtain color representations (Figure 3). Experiments show that color spatial location obtained via SPOT has a 100% accuracy.
3. We release the first meteorological VQA dataset, ClimateIQA. It consists of 8,760 high-resolution images and 254k instruction samples. Compiled from ERA5 (Hersbach et al., 2020) reanalysis data, data processed by SPOT, geography knowledge bases (Programme, 2019; Institute, 2018), and the Beaufort Scale (Monmonier, 2005), ClimateIQA is designed to train VLMs to identify extreme weather event, as well as interpret and describe meteorological heatmaps.
4. We introduce Climate-Zoo, the first collection of meteorological VLMs built upon state-of-the-art VLMs (e.g., Qwen-VL-Chat (Bai et al., 2023), Llava 1.6 (Liu et al., 2024b), and Yi-VL (Young et al., 2024)). Climate-Zoo substantially outperforms existing models on meteorological heatmap interpretation and can effectively localize areas of extreme weather events, setting a new benchmark for meteorological AI tools.

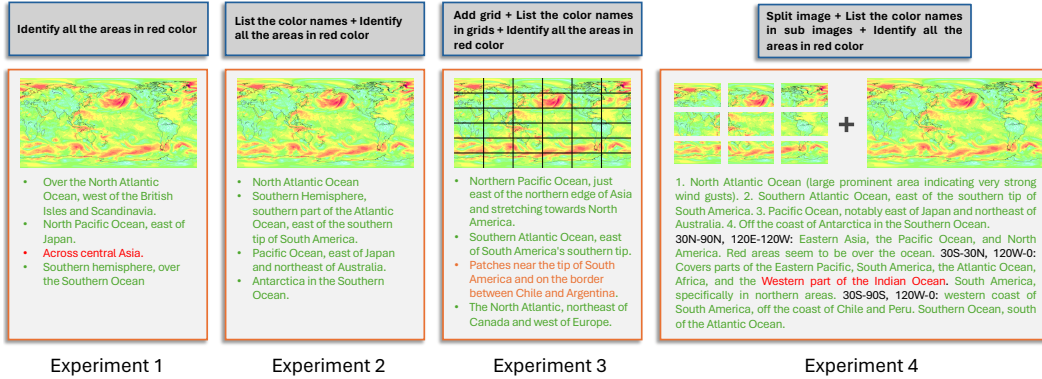


Figure 2: Result of the Initial Assessment via Prompt-Tuning GPT-4-Vision. Sentences in red mark inaccurate responses, sentences in orange and black mean surprising findings (patches and geography coordinates), and sentences in green mark accurate answers.

2 Related work

2.1 Vision language models and visual question answering

The integration of visual and textual data has led to the development of advanced VLMs, which typically build upon the capabilities of text-only LLMs, such as GPT-4 (Achiam et al., 2023), LLaMA (Touvron et al., 2023), Gemini (Team et al., 2023), and Claude (Anthropic, 2024). Notable developments in VLMs include GPT-4-vision (Achiam et al., 2023), QWEN-VL (Bai et al., 2023), and LLaVA (Li et al., 2024), which have substantially enhanced the efficiency of VQA tasks. These tasks require models to comprehend and respond to information and questions in both visual and textual formats.

To enhance model performance in VQA, researchers have adopted advanced methods for visual feature extraction (Zheng et al., 2023), developed robust model architectures (Liu et al., 2024b), and explored innovative learning paradigms (Chen et al., 2024). Despite these advancements, VQA tasks continue to face challenges, such as the occurrence of hallucinations (Bai et al., 2024), often stemming from issues like data quality and visual uncertainty (Leng et al., 2023). Addressing these issues highlights the critical need for high-quality datasets and effective strategies to mitigate challenges in VQA tasks.

2.2 AI for meteorology

The integration of AI in meteorology has seen many applications, such as employing AI for long-term weather prediction (Lam et al., 2022), typhoon trajectory forecasting (Bi et al., 2022), and weather classification (Dalal et al., 2023). The advent of LLMs like ClimSight (Koldunov and Jung, 2024), ChatClimate (Vaghefi et al., 2023), Arabic Mini-ClimateGPT (Mullappilly et al., 2023), and ClimateGPT (Thulke et al., 2024) has broadened the scope of textual data processing in meteorology. These models have been instrumental in assimilating general meteorological knowledge related to climates, answering common queries, and offering insights. However, these models predominantly rely on textual data. This becomes particularly limiting when addressing complex challenges such as the analysis of extreme weather event distributions, where textual data alone proves inadequate and prone to inaccuracies, often leading to serious hallucinations (Bulian et al., 2023). Meteorologists often need to interpret data from satellite images (Liu et al., 2024a), radar (Guastavino et al., 2022), heatmaps (Lee et al., 2024), and isobaric maps (Xu et al., 2024) to make accurate assessments. Nonetheless, there remains a lack of VLMs capable of interpreting such visual meteorological data.

3 Initial assessment of GPT-4-Vision

Among various VLMs, GPT-4-Vision (Achiam et al., 2023) has demonstrated exceptional capabilities in understanding and generating visual and textual content (Singh et al., [n. d.]). We began with an

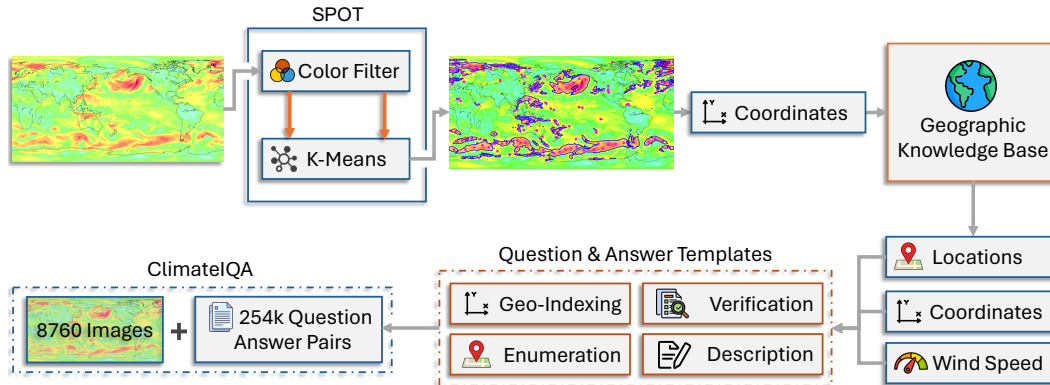


Figure 3: Dataset Creation Process. Images were processed using SPOT to extract color contours (marked in blue) and representative point coordinates (marked in purple), such as (-40, 65). The extracted data were integrated into geographic knowledge bases to retrieve location-specific information. These data, including location, coordinates, and wind speed, were then input into predefined question-and-answer templates, resulting in the generation of 254,040 question-answer pairs. The final dataset, ClimateQA, pairs these QA pairs with 8,760 images, enabling comprehensive climate-related visual question answering.

in-depth evaluation of its ability to identify and localize red regions in heatmap images, indicating areas like high wind speed, temperatures, or significant weather metrics, aiming to pinpoint areas for enhancement based on its limitations. Four experiments were designed for this assessment (Figure 2):

1. Direct Red Region Identification: We tested the VLM’s ability to identify red regions directly, without guidance, to evaluate its color perception and localization capabilities.
2. Two-Step Color Identification: After observing potential color confusion in the first experiment, the process was altered to first list all colors in the image, then identify red regions specifically, improving the accuracy of color recognition.
3. Grid-Based Color Identification: To capture fine-grained details, we implemented a grid-based method, dividing images into a 6×6 grid, each with geographic details. The model identified the color of each cell and then located the red-colored regions, evaluating the model’s ability to capture local color information and its impact on localization accuracy.
4. Image Segmentation and Combined Analysis: Employing image segmentation via the PIL toolkit (Umesh, 2012), we divided the input image into sub-images and tasked the VLM with analyzing both the overall and segmented images. The results were then combined for a comprehensive interpretation, aiming to improve the completeness and accuracy of the model’s responses.

The results varied across experiments. In Experiment 1, GPT-4-Vision struggled with direct identification of red regions, inaccurately marking locations such as "Across central Asia". Experiment 2 showed improvement with correct identifications, though responses were incomplete and the recall rate was just 5%. Experiment 3, the grid-based approach, better-captured details like patches but had inconsistent performance across different images, with an average accuracy of 7%. Experiment 4, using segmented and combined analysis, produced the most accurate results, successfully identifying sub-image colors and providing more complete interpretations, though it still exhibited geographical inaccuracies.

Overall, these experiments highlight areas for improvement in VLMs, particularly in addressing color confusion and enhancing geographical knowledge. Despite improvements in image segmentation and combined analysis, further refinements are necessary for more accurate and reliable performance in identifying and localizing colored regions in images.

4 ClimateQA dataset creation

As shown in Figure 3, we ensured the reliability of the image sources and developed a new method for accurately extracting color and position information from the images.

4.1 Data collection and pre-processing

Our meteorological data were derived from the ERA5 hourly dataset on single levels. ERA5, produced by the European Centre for Medium-Range Weather Forecasts (ECMWF) (Hersbach et al., 2020), provides comprehensive global climate and weather records since 1940. This dataset is created using data assimilation techniques that integrate model outputs with observational data, enhancing accuracy by reconciling forecasts with new observations every 12 hours. For this study, we selected hourly wind gust data for 2023. Due to the complexity of wind gust heatmaps, wind gust data is especially representative for identifying extreme weather. The method developed with wind gust data can be conveniently extended in the future to analyze less complex heatmaps, such as heatmaps for heatwaves, droughts, and heavy precipitation.

To classify wind speeds, we employed the Beaufort Scale (Monmonier, 2005), a widely recognized system that quantifies wind speed by observing its impact at sea or on land. The Beaufort Scale categorizes wind speeds from 0 to 12, with each level associated with a specific wind speed range and descriptive physical conditions. In our analysis, each wind force level is represented by a unique color gradient, starting from white for the lowest wind speeds and progressing through light cyan, aquamarine, light green, light lime green, light lemon yellow, light yellow, peach, light coral, salmon, deep pink, and dark magenta, culminating at dark purple for the highest wind speeds. To facilitate the geographical localization of extreme weather phenomena, we superimposed a world map onto each heatmap.

To extract and compile color information from meteorological heatmap images, we developed a method called "SPOT" (Sparse Position and Outline Tracking). Following the steps, we first extract contours of four base colors: red, yellow, white, and green with OpenCV (Culjak et al., 2012) as the color filter. Then, we acquire the contour coordinates of each color region to mitigate the issue of the irregular shapes of color regions in the heatmaps. Due to the massive volume of contour coordinate data, we represent each color region's geographical location and distribution shape through a minimal set of points. This process began with determining the number of points needed to represent the entirety of a color region based on its area within an image. However, representing irregularly shaped color regions with a few coordinate points is challenging, so we applied the K-Means clustering algorithm (Krishna and Murty, 1999) to calculate the centroid coordinates (the number of clusters determined by color region areas) for each color region. Simultaneously, we established a rule to remove any points located outside the color region and replace them with new points, ensuring that every point falls within the color region. As illustrated in Figure 3, each purple dot represents the position and shape of its corresponding color region. With the help of the SPOT method, we can correctly identify the spatial location of different color regions with 100% accuracy. The pseudo-code of SPOT is in Appendix 1.

4.2 Creating instruction-tuning data

After identifying the representative points for each color block using SPOT, we indexed the corresponding geographical names of these points coordinates using two geographic databases: the IHO Sea Areas (Institute, 2018) and the World Bank-approved Administrative Boundaries (Programme, 2019). The IHO Sea Areas database delineates the boundaries of the world's major oceans and seas, while the World Bank-approved administrative boundaries database includes international borders, disputed areas, coastlines, lakes, and a usage guide.

We then designed templates for question and answer generation, ensuring that each question and answer pair would be generated based on the templates and could be substantiated by the data. These templates were then used to generate the question-answer pairs, forming the instruction-tuning data. All the templates are provided in Appendix 1 for reference. We divided all the instruction-tuning data into four different types: (1) Verification questions that determine whether a location has been affected by extreme weather events; (2) Enumeration questions that list all the places that have been impacted by an extreme weather event; (3) Geo-Indexing questions that provide the coordinates of a location that experienced extreme weather events; and (4) Description questions that provide a detailed description for the given image.

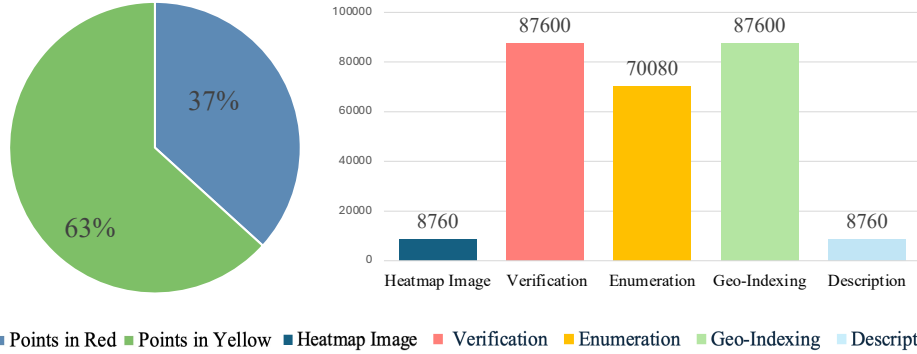


Figure 4: Distribution of red and yellow point coordinate data collected by SPOT (left) and the final ClimateQA dataset (right).

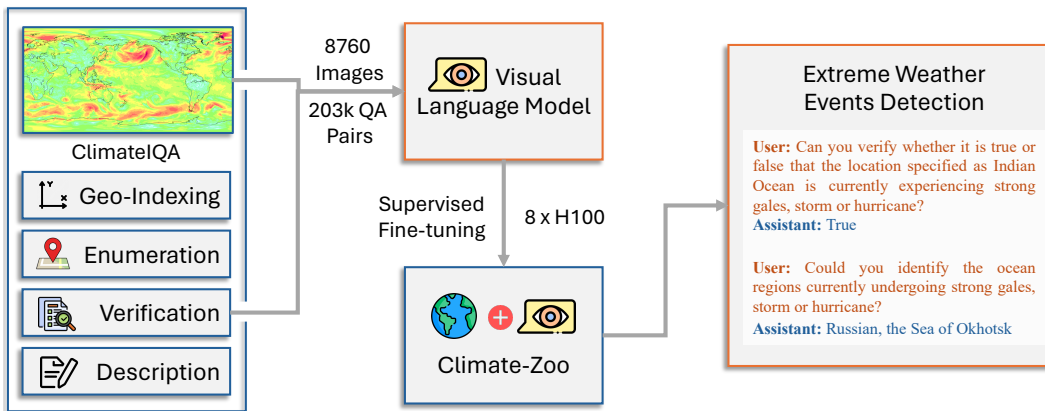


Figure 5: Process Supervised Fine-tuning Climate-Zoo.

4.3 Dataset statistics

Our approach produced 8,760 high-resolution heatmaps, each measuring 3510×1755 pixels. These images provide detailed visual representations of global wind patterns. An example of instruction-tuning data is shown in Figure 6. With geographical names fixed (Figure 4), the question type distribution is as follows: Verification Questions (34.5%), List Questions (27.6%), Geo-Indexing Questions (34.5%), and Description Questions (3.4%). We focused on localizing extreme weather, collecting points in red (wind speeds exceeding 20.8 m/s) and yellow (wind speeds between 10.8-20.7 m/s). Of the data collected by SPOT, 37% of the points are red, and 63% are yellow.

This process yielded a large-scale instruction-tuning dataset of 254,040 data points. We further split it into training, validation, and testing sets in a 7:1:2 ratio, with 177,828 instruction samples for training, 25,404 for validation, and 50,808 for testing. We designate 203k, including both training and validation data, as fine-tuning dataset.

5 Climate-Zoo: Adapting VLMs to meteorology

This section details our methods to enhance the performance of VLMs on EWED through prompt-tuning and supervised fine-tuning with ClimateQA.

Base models Based on model performance on VLM benchmarks (Goyal et al., 2017; Lu et al., 2022), we selected three state-of-the-art VLMs as our base models for improvement: Llava-v1.6-mistral-7b (Liu et al., 2024b), Qwen-VL-Chat (Bai et al., 2023), and Yi-VL-6B (Young et al., 2024). Llava-v1.6 excels in multimodal understanding, Qwen-VL-Chat in visual dialog tasks, and Yi-VL-6B in visual reasoning.

Supervised fine-tuning During the fine-tuning process shown in Figure 5, we strategically froze the weights of the visual encoder to reduce computational costs and mitigate the risk of overfitting. This decision is supported by research (Khattak et al., 2023) indicating that pre-trained visual encoders are already proficient in extracting meaningful features. Consequently, further fine-tuning on a single meteorological dataset might lead to overfitting. By keeping the visual encoder fixed, we preserved the generalization capability of the visual representations.

Training details We conducted full-parameter training on three prominent large-scale VLMs: Llava-v1.6 (7B parameters), Qwen-VL-Chat (7B parameters), and Yi-VL-6B (6B parameters), utilizing the Swift toolkit for its efficiency and flexibility. In addition to full-parameter tuning, we also fine-tune these models with Low-Rank Adaptation (LoRA) layers to further improve their adaptability. LoRA introduces a low-rank decomposition of the model’s weight matrices, allowing efficient adaptation to new tasks with minimal additional parameters. By setting the LoRA rank to 8, with an alpha value of 32 and a dropout probability of 0.05, we balance adaptation capacity and computational efficiency.

To expedite the training process, we employed 8 H100 80G GPUs and utilized Distributed Data Parallel along with DeepSpeed. The batch size was set to 1, and the learning rate was 0.0001 (1e-4). The entire experiment was conducted for a single epoch, spanning a total duration of 22 days.

6 Evaluation

6.1 Metrics

We designed a comprehensive framework to assess the performance of the models across four categories of questions. Our goal was to understand the model’s adaptability and accuracy across varied tasks. Below, we detail our methodological approach and assessment metrics.

F1 Score For Verification Questions, we evaluate the model’s ability to judge the correctness of statements using recall, precision, and F1 score (the harmonic mean of precision and recall).

Element Match Score For Enumeration Questions, we compute a match score (MS) between ground truth (x) and model-generated answer (y). It calculates correct matches via set intersection size and incorrect matches via symmetric differences. If this union size of both (x) and (y) is zero, the match score is zero. Otherwise, the score ranges from -1 to 1, with higher values indicating fewer hallucinations and more complete answers. The score is determined by the formula:

$$MS = \begin{cases} 0, & \text{if } |x \cup y| = 0 \\ \frac{|x \cap y| - (|x - y| + |y - x|)}{|x \cup y|}, & \text{otherwise} \end{cases} \quad (1)$$

Haversine Distance For Geo-indexing Questions, which involve determining precise geographical coordinates, we utilized the Haversine distance formula. This metric accurately measures the distance between model-generated coordinates (lat_m, lon_m) and ground truth coordinates (lat_g, lon_g) by accounting for the Earth’s curvature. The formula is as follows, where r represents the Earth’s radius:

$$d = 2r \cdot \arcsin\left(\sqrt{\sin^2\left(\frac{lat_m - lat_g}{2}\right) + \cos(lat_m) \cdot \cos(lat_g) \cdot \sin^2\left(\frac{lon_m - lon_g}{2}\right)}\right) \quad (2)$$

BLEU, ROUGE and GPT-4 Scores For Description Questions, we employ average BLEU and ROUGE and GPT-4 scores. BLEU-1 and BLEU-2 measure linguistic accuracy by comparing n-grams between the generated and ground truth descriptions. ROUGE-1, ROUGE-2, and ROUGE-L assess the overlap of n-grams, word sequences, and word pairs, offering insights into the comprehensiveness and relevance of the generated descriptions. Additionally, GPT-4 evaluates the overall quality and similarity of model-generated descriptions to ground truth answers on a five-point Likert scale. The prompt is shown in Appendix 7.

6.2 Results and analysis

Supervised fine-tuning Table 1 illustrates the outcomes of our experiments, highlighting that Climate-Zow models outperform all baseline models across various metrics. Specifically, for verification and enumeration questions, the baseline models were unable to provide answers, which is

Table 1: Result of Supervised Fine-tuning

	Model	F1 Score	Element Match Score	Haversine Distance 10 ³	BLEU	ROUGE	GPT4-Score (Similarity)	GPT4-Score (Total)
Baseline Model	Qwen-VL-Chat	0	-1	6.928	0	0.08	1	1.455
	Yi-VL-6B	0	-1	6.718	0.004	0.052	2	3.035
	Llava-v1.6-mistral-7b	0	-1	8.566	0	0.041	1.988	3.100
	GPT-4-Vision	0	-1	-	0	0	2.012	3.186
Climate-Zoo LoRa	Qwen-VL-Chat LoRa	0.909	-0.930	1.894	0.819	0.732	4.861	4.431
	Yi-VL-6B LoRa	0.905	-0.934	1.887	0.007	0.055	1.850	2.868
	Llava-v1.6-mistral-7b LoRa	0.910	-0.822	1.905	0.821	0.731	4.731	4.373
Climate-Zoo	Qwen-VL-Chat	0.910	-0.012	1.928	0.818	0.722	4.829	4.486
	Yi-VL-6B	0.912	-0.122	1.933	0.815	0.728	4.741	4.360
	Llava-v1.6-mistral-7b	0.897	-0.483	1.935	0.823	0.747	4.806	4.444

Table 2: Result of ablation study

Climate-Zoo Model	Dataset	F1 Score	Element Match Score	Haversine Distance 10 ³	BLEU	ROUGE	GPT4-Score (Similarity)	GPT4-Score (Total)
Yi-VL-6B	ClimateIQA-10k	0.909	-0.092	1.930	0.820	0.732	4.855	4.594
	ClimateIQA-50k	0.905	-0.070	1.943	0.820	0.728	4.687	4.422
	ClimateIQA-100k	0.912	-0.048	1.932	0.814	0.718	4.834	4.345
	ClimateIQA-203k	0.912	-0.122	1.933	0.815	0.728	4.741	4.360
Llava-v1.6-mistral-7b	ClimateIQA-10k	0.820	-0.913	6.335	0.611	0.624	4.631	4.508
	ClimateIQA-50k	0.825	-0.903	1.945	0.820	0.748	4.787	4.489
	ClimateIQA-100k	0.820	-0.532	1.972	0.825	0.750	4.662	4.394
	ClimateIQA-203k	0.897	-0.483	1.935	0.823	0.747	4.806	4.444

reflected in F1 scores of 0 and match scores of -1. In stark contrast, Climate-Zoo models demonstrated an impressive accuracy of around 90% in pinpointing regions affected by extreme weather, with the highest element match score reaching -0.012, indicating minimal inaccuracies in the data provided. Nevertheless, Climate-Zoo models did yield slightly incomplete lists of affected areas.

In tasks like geo-indexing and description questions, where baseline models did manage to generate responses, they were often plagued by significant errors. On the other hand, Climate-Zoo models significantly outperformed these baseline counterparts by delivering more precise coordinates and more accurate, rich descriptions, achieving superior BLEU, ROUGE, and GPT-4 scores.

While LoRA fine-tuning generally reduces the need for computational resources and, in specific cases like geo-indexing, even outperforms full parameter tuning, it doesn't universally enhance performance across all models. Notably, the Yi-VL-6B LoRA model falls short in handling description questions, underperforming both the fully fine-tuned models and the baseline.

Within the diverse ensemble of the Climate-Zoo collection, each model demonstrates particular strengths. The Qwen-VL-Chat model shines in delineating locations impacted by extreme weather events and providing detailed, vibrant image narratives, achieving high GPT scores. Conversely, the Yi-VL-6B model stands out with the highest F1 score, showcasing its accuracy in confirming extreme weather events at pinpoint locations. Meanwhile, the Llava-v1.6-mistral-7b model excels in spatial accuracy and textual richness, as evidenced by its exceptional performance in Haversine Distance, BLEU, and ROUGE evaluations, making it adept at generating precise coordinates and detailed visual descriptions.

Ablation study Table 2 presents the results of an ablation study using the Climate-Zoo models (Llava-v1.6-mistral-7b and Yi-VL-6B) with full parameters. This study evaluates model performance across varying dataset sizes: 10k, 50k, 100k, and 203k samples. Our findings reveal that increased data volume does not always correlate with improved model performance, with variations observed both between models and across different question types. At the model level, the Yi-VL-6B model achieves excellent results with just 10k samples; increasing the dataset size beyond this point can actually degrade its performance. In contrast, the Llava-v1.6-mistral-7b model shows improved performance with larger datasets. At the question type level, verification and enumeration questions demonstrate better performance with larger training datasets, whereas geo-indexing and description questions exhibit more variability.

Overall, the impact of dataset size on model performance varies significantly among different models. The Yi-VL-6B model appears especially suitable for industrial applications, as it can achieve high effectiveness with smaller datasets and fewer computational resources.

7 Limitations

We note that current VLMs in Climate-Zoo were trained on a subset of extreme weather events due to computational resource constraints. The heatmap’s red and yellow regions were included, while the green areas, containing over 500k samples, were excluded. Training one model on the full dataset would require nearly a month of computing time given our existing resources. Consequently, the model’s performance is suboptimal for the excluded green regions. With additional time and computational resources, we plan to retrain the model on the complete dataset in future work, which is expected to significantly improve accuracy and robustness, enabling better generalization across all geographic areas.

As we continue to develop and apply VLMs in the meteorology domain, it is essential to address potential ethical concerns for responsible deployment and beneficial outcomes. Misuse of these technologies could propagate disinformation, and inadequate auditing could lead to unfair decisions impacting specific groups. Vigilance in mitigating these issues is crucial.

8 Conclusions

This study presents pioneering work in integrating VLMs for EWED, providing a robust framework for extreme weather monitoring and prediction. Through a series of carefully designed experiments, we identified key issues of current general-purpose VLMs and proposed a framework of solutions to improve their performance. We introduced the SPOT method for precise color localization, developed ClimateIQA, the first large-scale dataset in this field, and established Climate-Zoo, a collection of state-of-the-art VLMs adapted for meteorological applications. Models based on Qwen-VL-Chat and Llava-v1.6-mistral-7b showed exceptional performance across verification, enumeration, geo-indexing, and description tasks of EWED. This research pushes the boundaries of AI usage in meteorology and contributes a benchmark for heatmap-based EWED, guiding future research to dive further into this field.

References

- Josh Achiam, Steven Adler, Sandhini Agarwal, Lama Ahmad, Ilge Akkaya, Florencia Leoni Aleman, Diogo Almeida, Janko Altenschmidt, Sam Altman, Shyamal Anadkat, et al. 2023. Gpt-4 technical report. *arXiv preprint arXiv:2303.08774* (2023).
- AI Anthropic. 2024. The claude 3 model family: Opus, sonnet, haiku. *Claude-3 Model Card* (2024).
- Jinze Bai, Shuai Bai, Shusheng Yang, Shijie Wang, Sinan Tan, Peng Wang, Junyang Lin, Chang Zhou, and Jingren Zhou. 2023. Qwen-vl: A frontier large vision-language model with versatile abilities. *arXiv preprint arXiv:2308.12966* (2023).
- Zechen Bai, Pichao Wang, Tianjun Xiao, Tong He, Zongbo Han, Zheng Zhang, and Mike Zheng Shou. 2024. Hallucination of Multimodal Large Language Models: A Survey. *arXiv preprint arXiv:2404.18930* (2024).
- Kaifeng Bi, Lingxi Xie, Hengheng Zhang, Xin Chen, Xiaotao Gu, and Qi Tian. 2022. Pangu-weather: A 3d high-resolution model for fast and accurate global weather forecast. *arXiv preprint arXiv:2211.02556* (2022).
- Jannis Bulian, Mike S Schäfer, Afra Amini, Heidi Lam, Massimiliano Ciaramita, Ben Gaiarin, Michelle Chen Huebscher, Christian Buck, Niels Mede, Markus Leippold, et al. 2023. Assessing Large Language Models on Climate Information. *arXiv preprint arXiv:2310.02932* (2023).
- Liangyu Chen, Bo Li, Sheng Shen, Jingkang Yang, Chunyuan Li, Kurt Keutzer, Trevor Darrell, and Ziwei Liu. 2024. Large language models are visual reasoning coordinators. *Advances in Neural Information Processing Systems* 36 (2024).
- Ivan Culjak, David Abram, Tomislav Pribanic, Hrvoje Dzapo, and Mario Cifrek. 2012. A brief introduction to OpenCV. In *2012 proceedings of the 35th international convention MIPRO*. IEEE, 1725–1730.

- Surjeet Dalal, Bijeta Seth, Magdalena Radulescu, Teodor Florin Cilan, and Luminita Serbanescu. 2023. Optimized deep learning with learning without forgetting (LwF) for weather classification for sustainable transportation and traffic safety. *Sustainability* 15, 7 (2023), 6070.
- Wei Fang, Qiongying Xue, Liang Shen, and Victor S Sheng. 2021. Survey on the application of deep learning in extreme weather prediction. *Atmosphere* 12, 6 (2021), 661.
- Yash Goyal, Tejas Khot, Douglas Summers-Stay, Dhruv Batra, and Devi Parikh. 2017. Making the v in vqa matter: Elevating the role of image understanding in visual question answering. In *Proceedings of the IEEE conference on computer vision and pattern recognition*. 6904–6913.
- Sabrina Guastavino, Michele Piana, Marco Tizzi, Federico Cassola, Antonio Iengo, Davide Sacchetti, Enrico Solazzo, and Federico Benvenuto. 2022. Prediction of severe thunderstorm events with ensemble deep learning and radar data. *Scientific Reports* 12, 1 (2022), 20049.
- Hans Hersbach, Bill Bell, Paul Berrisford, Shoji Hirahara, András Horányi, Joaquín Muñoz-Sabater, Julien Nicolas, Carole Peubey, Raluca Radu, Dinand Schepers, et al. 2020. The ERA5 global reanalysis. *Quarterly Journal of the Royal Meteorological Society* 146, 730 (2020), 1999–2049.
- Flanders Marine Institute. 2018. Marine Regions. <https://www.marineregions.org/sources.php>
- Muhammad Uzair Khattak, Syed Talal Wasim, Muzammal Naseer, Salman Khan, Ming-Hsuan Yang, and Fahad Shahbaz Khan. 2023. Self-regulating prompts: Foundational model adaptation without forgetting. In *Proceedings of the IEEE/CVF International Conference on Computer Vision*. 15190–15200.
- Nikolay Koldunov and Thomas Jung. 2024. Local climate services for all, courtesy of large language models. *Communications Earth & Environment* 5, 1 (2024), 13.
- K Krishna and M Narasimha Murty. 1999. Genetic K-means algorithm. *IEEE Transactions on Systems, Man, and Cybernetics, Part B (Cybernetics)* 29, 3 (1999), 433–439.
- Remi Lam, Alvaro Sanchez-Gonzalez, Matthew Willson, Peter Wirnsberger, Meire Fortunato, Ferran Alet, Suman Ravuri, Timo Ewalds, Zach Eaton-Rosen, Weihua Hu, et al. 2022. GraphCast: Learning skillful medium-range global weather forecasting. *arXiv preprint arXiv:2212.12794* (2022).
- Juhyun Lee, Jungho Im, and Yeji Shin. 2024. Enhancing tropical cyclone intensity forecasting with explainable deep learning integrating satellite observations and numerical model outputs. *iScience* (2024).
- Sicong Leng, Hang Zhang, Guanzheng Chen, Xin Li, Shijian Lu, Chunyan Miao, and Lidong Bing. 2023. Mitigating object hallucinations in large vision-language models through visual contrastive decoding. *arXiv preprint arXiv:2311.16922* (2023).
- Chunyuan Li, Cliff Wong, Sheng Zhang, Naoto Usuyama, Haotian Liu, Jianwei Yang, Tristan Naumann, Hoifung Poon, and Jianfeng Gao. 2024. Llava-med: Training a large language-and-vision assistant for biomedicine in one day. *Advances in Neural Information Processing Systems* 36 (2024).
- Haotian Liu, Chunyuan Li, Qingyang Wu, and Yong Jae Lee. 2024b. Visual instruction tuning. *Advances in neural information processing systems* 36 (2024).
- Renfeng Liu, Haonan Dai, YingYing Chen, Hongxing Zhu, DaiHeng Wu, Hao Li, Dejun Li, and Cheng Zhou. 2024a. A study on the DAM-EfficientNet hail rapid identification algorithm based on FY-4A_AGRI. *Scientific Reports* 14, 1 (2024), 3505.
- Pan Lu, Swaroop Mishra, Tanglin Xia, Liang Qiu, Kai-Wei Chang, Song-Chun Zhu, Oyvind Tafjord, Peter Clark, and Ashwin Kalyan. 2022. Learn to explain: Multimodal reasoning via thought chains for science question answering. *Advances in Neural Information Processing Systems* 35 (2022), 2507–2521.

- Mark Monmonier. 2005. Defining the wind: The Beaufort scale, and how a 19th century admiral turned science into poetry.
- Sahal Mullappilly, Abdelrahman Shaker, Omkar Thawakar, Hisham Cholakkal, Rao Anwer, Salman Khan, and Fahad Khan. 2023. Arabic Mini-ClimateGPT: A Climate Change and Sustainability Tailored Arabic LLM. In *Findings of the Association for Computational Linguistics: EMNLP 2023*. 14126–14136.
- World Food Programme. 2019. World Administrative Boundaries - Countries and Territories. <https://public.opendatasoft.com/explore/dataset/world-administrative-boundaries/information/>
- Evan Racah, Christopher Beckham, Tegan Maharaj, Samira Ebrahimi Kahou, Mr Prabhat, and Chris Pal. 2017. Extremeweather: A large-scale climate dataset for semi-supervised detection, localization, and understanding of extreme weather events. *Advances in neural information processing systems* 30 (2017).
- Kunal Singh, Mukund Khanna, Ankan Biswas, Pradeep Moturi, et al. [n. d.]. VISUAL PROMPTING METHODS FOR GPT-4V BASED ZERO-SHOT GRAPHIC LAYOUT DESIGN GENERATION. In *The Second Tiny Papers Track at ICLR 2024*.
- Gemini Team, Rohan Anil, Sebastian Borgeaud, Yonghui Wu, Jean-Baptiste Alayrac, Jiahui Yu, Radu Soricut, Johan Schalkwyk, Andrew M Dai, Anja Hauth, et al. 2023. Gemini: a family of highly capable multimodal models. *arXiv preprint arXiv:2312.11805* (2023).
- David Thulke, Yingbo Gao, Petrus Pelsler, Rein Brune, Rricha Jalota, Floris Fok, Michael Ramos, Ian van Wyk, Abdallah Nasir, Hayden Goldstein, et al. 2024. ClimateGPT: Towards AI Synthesizing Interdisciplinary Research on Climate Change. *arXiv preprint arXiv:2401.09646* (2024).
- Hugo Touvron, Thibaut Lavril, Gautier Izacard, Xavier Martinet, Marie-Anne Lachaux, Timothée Lacroix, Baptiste Rozière, Naman Goyal, Eric Hambro, Faisal Azhar, et al. 2023. Llama: Open and efficient foundation language models. *arXiv preprint arXiv:2302.13971* (2023).
- P Umesh. 2012. Image processing in python. *CSI Communications* 23, 2 (2012), 23–24.
- Saeid Ashraf Vaghefi, Dominik Stammach, Veruska Muccione, Julia Bingler, Jingwei Ni, Mathias Kraus, Simon Allen, Chiara Colesanti-Senni, Tobias Wekhof, Tobias Schimanski, et al. 2023. ChatClimate: Grounding conversational AI in climate science. *Communications Earth & Environment* 4, 1 (2023), 480.
- Andreas Wunsch, Tanja Liesch, and Stefan Broda. 2022. Deep learning shows declining groundwater levels in Germany until 2100 due to climate change. *Nature communications* 13, 1 (2022), 1221.
- Jing Xu, Ping Zhao, Johnny CL Chan, Mingyuan Shi, Chi Yang, Siyu Zhao, Ying Xu, Junming Chen, Ling Du, Jie Wu, et al. 2024. Increasing tropical cyclone intensity in the western North Pacific partly driven by warming Tibetan Plateau. *Nature Communications* 15, 1 (2024), 310.
- Alex Young, Bei Chen, Chao Li, Chengen Huang, Ge Zhang, Guanwei Zhang, Heng Li, Jiangcheng Zhu, Jianqun Chen, Jing Chang, et al. 2024. Yi: Open foundation models by 01. ai. *arXiv preprint arXiv:2403.04652* (2024).
- Sungduk Yu, Walter Hannah, Liran Peng, Jerry Lin, Mohamed Aziz Bhourri, Ritwik Gupta, Björn Lütjens, Justus C Will, Gunnar Behrens, Julius Busecke, et al. 2024. ClimSim: A large multi-scale dataset for hybrid physics-ML climate emulation. *Advances in Neural Information Processing Systems* 36 (2024).
- Dehua Zheng, Xiaochen Zheng, Laurence T Yang, Yuan Gao, Chenlu Zhu, and Yiheng Ruan. 2023. Mffn: Multi-view feature fusion network for camouflaged object detection. In *Proceedings of the IEEE/CVF Winter Conference on Applications of Computer Vision*. 6232–6242.

Checklist

1. For all authors...
 - (a) Do the main claims made in the abstract and introduction accurately reflect the paper’s contributions and scope? [Yes]
 - (b) Did you describe the limitations of your work? [Yes]
 - (c) Did you discuss any potential negative societal impacts of your work? [Yes]
 - (d) Have you read the ethics review guidelines and ensured that your paper conforms to them? [Yes]
2. If you are including theoretical results...
 - (a) Did you state the full set of assumptions of all theoretical results? [N/A]
 - (b) Did you include complete proofs of all theoretical results? [N/A]
3. If you ran experiments (e.g. for benchmarks)...
 - (a) Did you include the code, data, and instructions needed to reproduce the main experimental results (either in the supplemental material or as a URL)? [Yes]
 - (b) Did you specify all the training details (e.g., data splits, hyperparameters, how they were chosen)? [Yes]
 - (c) Did you report error bars (e.g., with respect to the random seed after running experiments multiple times)? [Yes] *We report error bars for only one model due to the high computational expense of calculating error bars for all models. The error bar is shown in the supplementary materials.*
 - (d) Did you include the total amount of compute and the type of resources used (e.g., type of GPUs, internal cluster, or cloud provider)? [Yes]
4. If you are using existing assets (e.g., code, data, models) or curating/releasing new assets...
 - (a) If your work uses existing assets, did you cite the creators? [Yes]
 - (b) Did you mention the license of the assets? [Yes]
 - (c) Did you include any new assets either in the supplemental material or as a URL? [Yes]
 - (d) Did you discuss whether and how consent was obtained from people whose data you’re using/curating? [Yes]
 - (e) Did you discuss whether the data you are using/curating contains personally identifiable information or offensive content? [Yes]
5. If you used crowdsourcing or conducted research with human subjects...
 - (a) Did you include the full text of instructions given to participants and screenshots, if applicable? [N/A]
 - (b) Did you describe any potential participant risks, with links to Institutional Review Board (IRB) approvals, if applicable? [N/A]
 - (c) Did you include the estimated hourly wage paid to participants and the total amount spent on participant compensation? [N/A]

A Appendix

A.1 License

The ClimateIQA dataset and Climate-Zoo will be publicly available and use the **CC BY 4.0 license**.

The IHO Sea Area and the World Bank-approved Administrative Boundaries datasets, used to create ClimateIQA, are licensed under **CC BY 4.0 license**.

The ERA5 dataset is available under a free, worldwide, non-exclusive, royalty-free, and perpetual license. According to this license, access to Copernicus Products is granted for any lawful purpose. Permissible uses include, but are not limited to, reproduction, distribution, public communication, adaptation, modification, and combination with other data and information.

A.2 Example of question types

The following Figure 6 shows the four question types in the ClimateIQA instruction tuning data.

Conversation

Enumeration Question: Could you identify the ocean regions currently undergoing strong gales, storm or hurricane?

Assistant: High Seas of the North Atlantic Ocean: Canary Islands, Southern Peninsula Brazilian (Trindade) part of the South Atlantic Ocean: Alagoas Russian part of the Sea of Okhotsk: Magadan New Zealand.

Verification Question: Can you verify whether it is true or false that the location specified as High Seas of the Indian Ocean is currently experiencing strong gales, storm or hurricane?

Assistant: True

Specific Information Question : What is the latitude and longitude of the location referred to as Seychellois part of the Indian Ocean?

Assistant: (-4.97, 52.31)

Description Question : Can you describe the image in detail?

Assistant: Globally, regions are battling intense weather phenomena, including powerful gales, storms, and hurricanes, with wind gusts surpassing 20.7 m/s. The fury of these winds is felt over vast lands and oceanic stretches alike. Notably, areas such as High Seas of the North Atlantic Ocean, Brazilian (Trindade) part of the South Atlantic Ocean ... Closer to human habitation, land regions in South America, Western Europe ... Moreover, a vast array of regions encounters strong breezes and winds gusting between 10.8 to 20.7 m/s, impacting both land and sea. This includes High Seas of the North Atlantic Ocean ... On land, South America, Western Europe ... each face their own challenges with these forceful winds that spare few corners of the Earth.

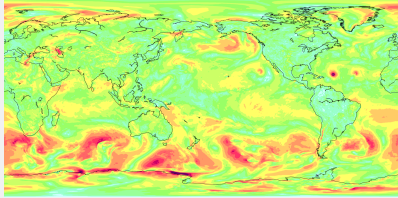


Figure 6: Example of Visual Question Answering Question Types in the Climate Domain.

A.3 Answer generated in preliminary study

Table 3: An Example of Experiment One

Prompt	This is a global wind gust heatmap. Could you please identify the areas are red color?
Answer	Based on the colors on this global wind gust map, the red areas, which typically indicate regions of higher wind gusts, appear in several locations. Here are the general areas where red coloration is present: 1. Over the North Atlantic Ocean, west of the British Isles and Scandinavia, indicating a zone of high wind gust activity possibly associated with a storm system. 2. In the North Pacific Ocean, east of Japan, which might be showing strong wind gusts also associated with a storm system. 3. Across central Asia, which could be indicative of strong winds blowing over the steppes or associated with a weather system in the region. 4. A region in the southern hemisphere, possibly over the Southern Ocean, indicating strong wind gusts which are common in those latitudes known as the roaring forties and furious fifties. It's important to note that without a legend or scale, the exact wind speeds corresponding to the red color cannot be determined.

Table 4: An Example of Experiment Two

Prompt	This is a global wind gust heatmap. please list the color name in the image. Could you please identify the areas are red color?
Answer	<p>The image shows different colors representing varying wind gust intensities across the globe. Here are the prominent colors visible in the image:</p> <ol style="list-style-type: none">1. Green - varying shades indicating moderate wind gusts.2. Yellow - indicating stronger wind gusts compared to green areas.3. Orange - indicating even stronger wind gusts, higher than yellow areas.4. Red - representing the strongest wind gusts visible on the map. <p>As for the red areas:</p> <ul style="list-style-type: none">- There is a large, prominent red area over the North Atlantic Ocean, indicating very strong wind gusts there.- In the Southern Hemisphere, another visible red area is over the southern part of the Atlantic Ocean, east of the southern tip of South America.- There are also red areas in the Pacific Ocean, notably east of Japan and northeast of Australia.- Another notable red area is visible just off the coast of Antarctica in the Southern Ocean. <p>Keep in mind that identifying specific geographic locations just based on colors on a map can be challenging without specific map coordinates, country borders, or other geographical markers.</p>

Table 5: An Example of Experiment Three

Prompt	<p>This is a global wind gust heatmap. there are black grids in the image, from left to right is the longitude, there are 6 columns, each column stand for 0 60E,60E 120E,120E 180,180 120W, 120W 60W, 60W 0W. from bottom to top is the latitude, there are 6 rows, each row stands for 90S 60S, 60S 30S, 30S 0, 0 30N, 30N 60N, 60N 90N. Please list the color name in each grid. Could you please based on the color name in grids identify all the areas in red color?</p>
Answer	<p>Here are the predominant color names in each grid, starting from the leftmost column (0 60E) to the rightmost column (60W 0W) and from bottom to top (90S 60S to 60N 90N):</p> <ol style="list-style-type: none"> 0 60E - 90S 60S: Light green and yellow - 60S 30S: Green with patches of red and yellow - 30S 0: Yellow with areas of green and red - 0 30N: Green, yellow, and small areas of red - 30N 60N: Green transitioning to yellow and red - 60N 90N: Yellow and red with patches of green 60E 120E - 90S 60S: Light green and yellow - 60S 30S: Yellow with areas of red and green - 30S 0: Yellow and green with small patches of red - 0 30N: Green with some yellow - 30N 60N: Yellow and red with hints of green - 60N 90N: Green and yellow with small areas of red 120E 180 - 90S 60S: Light green and yellow - 60S 30S: Green and yellow with red areas - 30S 0: Yellow with areas of green and small patches of red - 0 30N: Green and yellow with hints of red - 30N 60N: Green and yellow with red areas - 60N 90N: Yellow with patches of red 180 120W - 90S 60S: Light green and yellow - 60S 30S: Light green - 30S 0: Green and yellow with areas of red - 0 30N: Green and yellow with small patches of red - 30N 60N: Green and yellow with areas of red - 60N 90N: Green and yellow 120W 60W - 90S 60S: Light green and yellow - 60S 30S: Green with patches of red and yellow - 30S 0: Green and yellow - 0 30N: Green and yellow - 30N 60N: Yellow and green with red areas - 60N 90N: Green and yellow with patches of red 60W 0W - 90S 60S: Light green and yellow - 60S 30S: Yellow and green with areas of red - 30S 0: Yellow with patches of green and red - 0 30N: Green and yellow with small areas of red - 30N 60N: Yellow and green with red areas - 60N 90N: Green and yellow with areas of red <p>The colors on a heatmap such as this generally range from cooler colors (like greens and blues) representing lower values to warmer colors (like yellows, oranges, and reds) representing higher values. Since there are no distinct boundaries, naming a single color for each grid would not be accurate.</p> <p>As for the red areas on the map, they indicate regions of high wind gusts. Describing their locations with precision is difficult because of the blending colors and the lack of borders on the map, but I can provide a general idea of where the reddest areas are:</p> <ol style="list-style-type: none"> A very intense red area is located in the Northern Pacific Ocean, just east of the northern edge of Asia and stretching towards North America. Another significant red area is in the southern Atlantic Ocean, east of South America's southern tip. There are patches of red near the tip of South America and on the border between Chile and Argentina. The North Atlantic, northeast of Canada and west of Europe, also contains some red areas.

A.4 Pseudo code of SPOT

Algorithm 1 SPOT: Sparse Position and Outline Tracking

Input: Image path img_path , color name $color_name$

Output: List of latitude and longitude coordinates

```
1: Initialize  $GetCoordinate$  with  $img\_path$ 
2: procedure GETCOLORBOUNDARIES( $image, color\_name$ )
3:   Convert  $image$  to HSV color space
4:   Generate mask based on color range for  $color\_name$ 
5:   Find contours in the mask
6:   return contours, mask
7: end procedure
8: procedure GETREPRESENTATIVEPOINTS( $image, contour, num\_points$ )
9:   Draw  $contour$  on a mask
10:  Erode the mask
11:  Find points in the eroded mask
12:  if number of points  $\leq num\_points$  then
13:    return points
14:  else
15:    Apply K-Means clustering to points to get  $num\_points$ 
16:    return cluster centers as representative points
17:  end if
18: end procedure
19: procedure PROCESS( $color\_name$ )
20:   $contours, mask \leftarrow GETCOLORBOUNDARIES(image, color\_name)$ 
21:  Calculate total area of selected regions in  $mask$ 
22:  for each  $contour$  in  $contours$  do
23:    Calculate  $area\_ratio$  for the contour
24:    Determine  $num\_points$  based on  $area\_ratio$ 
25:     $contour\_points \leftarrow GETREPRESENTATIVEPOINTS(image, contour, num\_points)$ 
26:    Annotate  $image$  with  $contour\_points$ 
27:  end for
28:  return points
29: end procedure
30: procedure CONVERTPOINTSTOCOORDINATES( $points$ )
31:  Initialize lists for longitude  $\lambda$  and latitude  $\varphi$ 
32:  for each point  $pt$  in  $points$  do
33:    Calculate longitude and latitude based on  $pt$  and image dimensions
34:    Append to  $\lambda$  and  $\varphi$  lists
35:  end for
36:  return  $\varphi, \lambda$ 
37: end procedure
38: procedure GETCOR( $color\_name$ )
39:   $points \leftarrow PROCESS(color\_name)$ 
40:   $\varphi, \lambda \leftarrow CONVERTPOINTSTOCOORDINATES(points)$ 
41:  Print image dimensions
42:  return  $\varphi, \lambda$ 
43: end procedure
```

A.5 Question and answer format template

Table 6: Template of Question and Answer Format

Question Type	Format	
Verification	Question	Can you verify whether it is true or false that the location specified as {Location Name} is currently experiencing strong gales, storm or hurricane?
	Answer	True/False
Enumeration	Question	Could you identify the { "Land" or "Ocean"} regions currently undergoing strong gales, storm or hurricane?
	Answer	{Continent Name or Ocean Name}; {Province or State Name}
Geo-Indexing	Question	What is the latitude and longitude of the location referred to as {Location Name} ?
	Answer	{Coordinate e.g.(-58.82, 176.31)}
Description	Question	Can you describe the image in detail?
	Answer	Globally, regions are battling intense weather phenomena, including powerful gales, storms, and hurricanes, with wind gusts surpassing 20.7 m/s. The fury of these winds is felt over vast lands and oceanic stretches alike. Notably, areas such as {Ocean Name in Red Color} . Closer to human habitation, land regions in {Land Name in Red Color} reel under the power of these gales, showing nature's unbridled force across both developed and developing landscapes. Moreover, a vast array of regions encounters strong breezes and winds gusting between 10.8 to 20.7 m/s, impacting both land and sea. This includes {Ocean Name in Yellow Color} . On land, {Land Name in Yellow Color} , each face their own challenges with these forceful winds that spare few corners of the Earth.

A.6 GPT-4 evaluation prompt

Table 7: GPT-4 Evaluation Prompt

Prompt	<p>The user question is {question}. the ground truth answer is {gt_ans}, the generated response {gpt_ans} is generated by GPT model.</p> <p>Please act as an impartial judge and evaluate the quality of the response provided by AI assistant to the question displayed upper! You should give three scores to the response. the highest score is 5 and the lowest score is 1. the scores include:</p> <p>Score 1: the total score considering factors helpfulness, relevance, accuracy, depth, creativity, and level of detail of the generated response.</p> <p>Score 2: the similarity and completeness score between ground truth answer and generated response. sometimes the generated answer have mention some inaccurate point or the answer is incomplete compared with the ground truth answer. 5 means 80%-90% similar. 4 means 60%-80% similar. 3 means 40%-60% similar, 2 means 20%-40% similar and 1 means 0-20% similar.</p> <p>Score 3: the total score considering factors helpfulness, relevance, accuracy, depth, creativity, and level of detail of the ground truth answer.</p> <p>Avoid any position biases and ensure that the order in which the responses were presented does not influence your decision. Do not allow the length of the responses to influence your evaluation, Be as objective as possible. Directly output the score and strictly follow the format:</p> <p>### Score 1: number ### Score 2: number ### Score 3: number</p>
---------------	---
